

Supporting Information

Organic-Inorganic Hybrids of Fe-Co Polyphenolic Networks Wrapped Fe₃O₄ Nanocatalysts for Significantly Enhanced Oxygen Evolution

Xin Jia,^a Jinzhu Wu,^b Ke Lu,^c Yang Li,^b Xianshu Qiao,^a Jacob Kaelin,^c Songtao Lu,^{*,a, b}

Yingwen Cheng,^{*,c} Xiaohong Wu,^b and Wei Qin ^{*,a}

^a School of Materials Science and Engineering, Harbin Institute of Technology, Harbin,

Heilongjiang, 150001, P. R. China. E-mail: qinwei@hit.edu.cn (W.Q.)

^b School of Chemistry and Chemical Engineering, Harbin Institute of Technology, Harbin,

Heilongjiang, 150001, P.R. China. E-mail: lusongtao@hit.edu.cn (S.L.)

^c Department of Chemistry and Biochemistry, Northern Illinois University, DeKalb, IL 60115

United States. E-mail: ycheng@niu.edu (Y.C.)

Materials and Methods

Chemicals and materials: Iron (III) chloride hexahydrate (AR, $\geq 98\%$), Cobalt(II) nitrate hexahydrate (AR, $\geq 98\%$), anhydrous sodium acetate (AR, $\geq 98\%$), 2-methylimidazole (AR, $\geq 98\%$), tannic acid (AR, $\geq 98\%$), iridium oxide (AR, $\geq 98\%$) were purchased from Aladdin, China. Perfluorosulfonic acid-PTEE copolymer (Nafion solution, 5%wt) was from Alfa Aesar. All the reagents were used as received without further purification. Nanopure water purified through a Millipore water purification system was used for all experiments.

Synthesis of Fe_3O_4 colloidal particles: In a typical protocol, 1.9 g of $\text{FeCl}_3 \cdot 6\text{H}_2\text{O}$ and 5.6 g of CH_3COONa were dissolved in 70 ml of ethylene glycol. The solution was transferred to a 50 ml Teflon-lined stainless steel autoclave container and reacted at 200 °C for 12 h. Afterwards the container was cooled to room temperature naturally and the produced solids were isolated from the solution via centrifugation at 5000 rpm for 10 min, and were washed with ethanol for 3 times and dried at 70 °C for 12 h.

Synthesis of ZIF-67@ Fe_3O_4 composite: 70 mg of the as-synthesized Fe_3O_4 NPs were dispersed in 25 ml methanol by sonication for 15 min. 330 mg of 2-methylimidazole was then dissolved in this solution and form the solution A. In a separate glass vial, 300 mg of $\text{Co}(\text{NO}_3)_2 \cdot 6\text{H}_2\text{O}$ was dissolved in 25 ml methanol to form the solution B. Solutions B was slowly injected to solution A and the remaining solution was stirred for 5 min, and ZIF-67@ Fe_3O_4 particles were obtained after aging at room temperature for 24 h. The produced solids were collected by centrifugation at 5000 rpm for 10 min and washed with ethanol 3 times, and dried at 70 °C for 12 h. These experiments were all performed in air.

Formation of CoFe-phenolic networks@Fe₃O₄ Core-Shell Structure: 20 mg of the as-synthesized ZIF-67@Fe₃O₄ polyhedrons were placed in 50 ml tannic acid solution (5 g/l, dissolved in methanol) and were aged under stirring for 30 min. Hybrid nanoparticles with core-shell structure were formed during this process and were collected by centrifugation at 5000 rpm for 10 min and washed with ethanol 3 times, and dried at 70 °C for 12 h. These experiments were all performed in air.

Materials characterization: Powder XRD patterns were collected on an Empyrean X-ray diffractometer equipped with a Cu K α radiation source ($\lambda = 0.154178$ nm). XPS measurements were performed using a Thermo Fischer ESCALAB 250Xi spectrophotometer with the excitation source of monochromatic aluminum. The structure and composition of the samples were studied by scanning electron microscopy (Merlin Compact SEM operated at 10-20 kV) and transmission electron microscopy (Tecnai G2 F30 TEM operated at 200 kV), along with energy dispersive X-ray (EDX) spectroscopy for both SEM and TEM. Fourier transform infrared spectroscopy (FTIR) spectra were acquired using a Nexus system. UV-vis absorption spectra were recorded using a METASH Model 8000 UV-vis spectrophotometer. The electrical conductivity was measured at room temperature using a Hall Effect Measurement System equipped with a four-point probe with the pattern of 5 mm \times 5 mm (SwimHALL 8800, Chinese Taipei). Samples were prepared by compressing the powders at 15 MPa using a die-set to thin discs. The BET surface area and pore size distribution were investigated by a Micromeritics TriStar II 3020 analyzer.

Electrochemical measurements: Linear sweep voltammetry (LSV), chronopotentiometric measurements and cyclic voltammetry (CV) measurements were carried out in 1 M KOH (pH 13.7) using a potentiostat (CHI660D, CH Instruments). All measurements were performed in a

three-electrode configuration at room temperature, using a saturated calomel electrode as the reference electrode and a graphite rod as the counter electrode. The working electrode was a glassy carbon electrode cased with the 20 μl of the catalyst ink, which was prepared by dispersing 5.0 mg catalyst in 1 ml methanol containing 0.1% Nafion and was sonicated for 2 h to form a homogeneous mixture. The catalyst loading was about 1.4 mg cm^{-2} . All potential measurements were converted to the RHE based on the following formula $E_{\text{RHE}} = E_{\text{SCE}} + 0.242 + 0.059 \text{ pH}$ (in volts). The overpotentials for oxygen evolution reaction were calculated according to the following formula: $\eta = E_{\text{RHE}} - 1.23 \text{ V}$. The electrochemical double-layer capacitance was determined from CV curves measured in the potential range according to the following equation: $C_{\text{dl}} = I_c/v$, where C_{dl} , I_c , and v are the double-layer capacitance (mF cm^{-2}) of the electroactive materials, charging current (mA cm^{-2}), and scan rate (mV s^{-1}), respectively. For LSV, the overpotential was swept from 1.0 to 1.7 V (vs. RHE) at a scan rate of 5 mVs^{-1} . EIS was recorded at 1.5 V (vs. RHE) using an AC voltage amplitude of 2 mV and a quiet time of 5 s. The frequency range investigated was from 0.1 Hz to 100 kHz. Chronopotentiometry was used to evaluate the catalytic stability; the current densities were set to 10 mA cm^{-2} and 50 mA cm^{-2} , respectively, and the potential was limited to 1.4 - 2.0 V (vs. RHE).

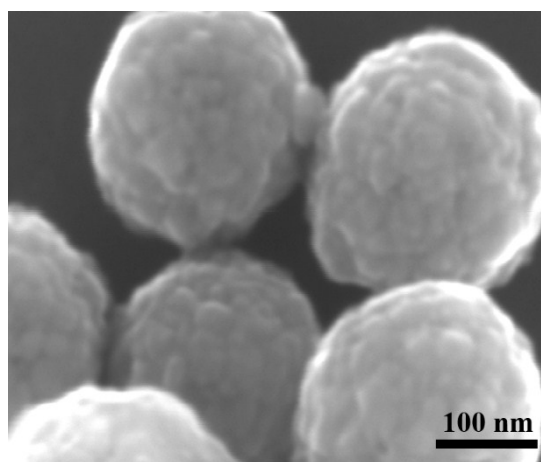


Figure S1: High resolution SEM image of as-synthesized Fe_3O_4 nanoparticles. These particles have diameters of approximately 200 nm and appeared as agglomerates of primary particles with

few nanometers.

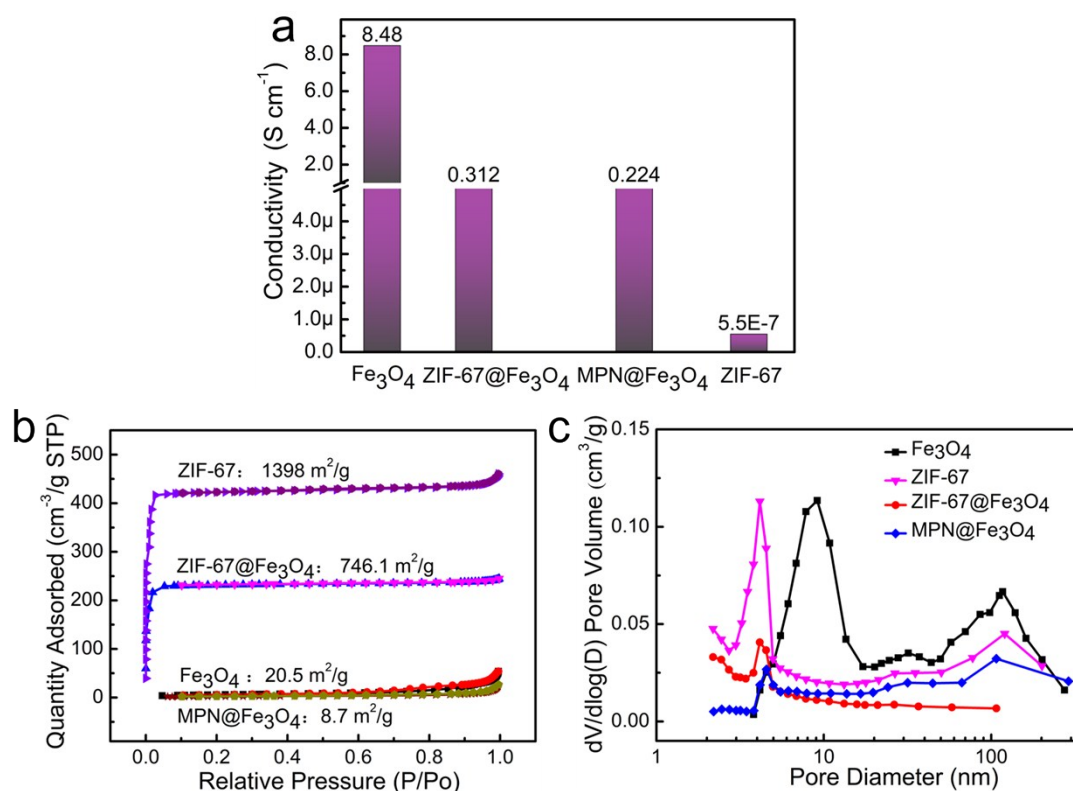


Figure S2: a) Comparison of the conductivity of Fe₃O₄, ZIF-67@Fe₃O₄, MPN@Fe₃O₄ NPs and ZIF-67; b) nitrogen adsorption/desorption isotherms and (c) BJH pore size distribution curves of MPN@Fe₃O₄, ZIF-67@Fe₃O₄, Fe₃O₄ NPs and ZIF-67.

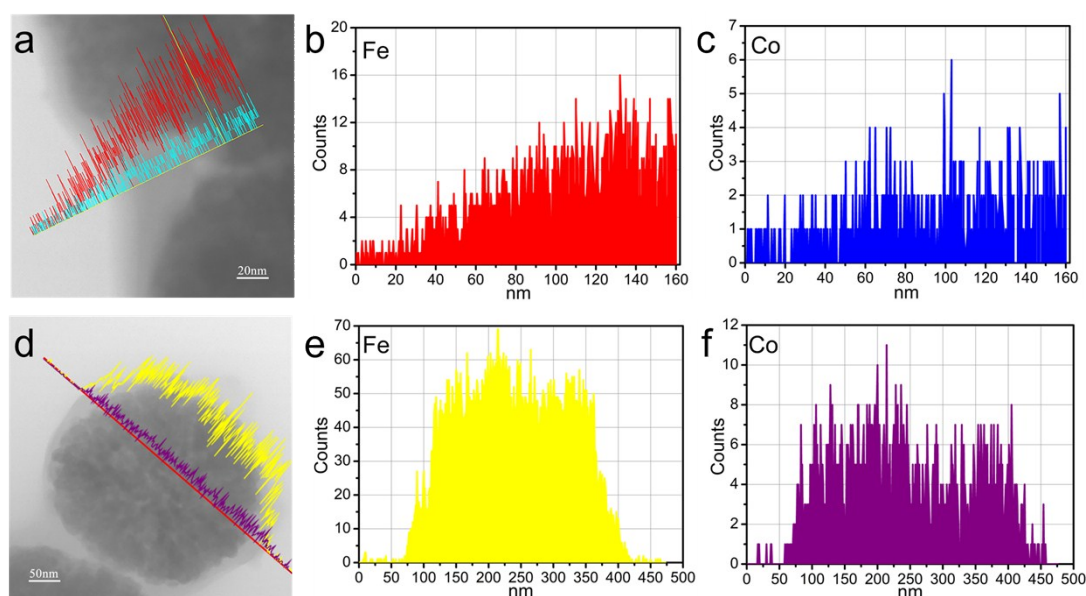


Figure S3. TEM image of the MPN@Fe₃O₄ nanoparticles. The presence of thin MPN shells and Fe/Co cations were clearly resolved for each particle.

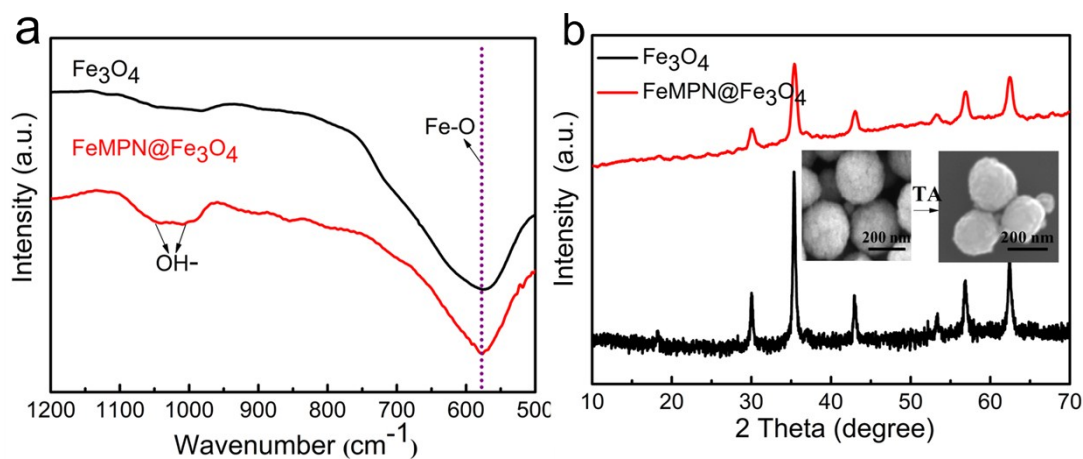


Figure S4: Structural characterization of FeMPN@Fe₃O₄ prepared by dispersing 20 mg Fe₃O₄ and 250 mg tannic acid in 50 ml methanol. The reaction time was 30 min. The results show formation of thin Fe-MPN layers (FT-IR and SEM) and the reduced crystallinity (XRD) after reaction with TA.

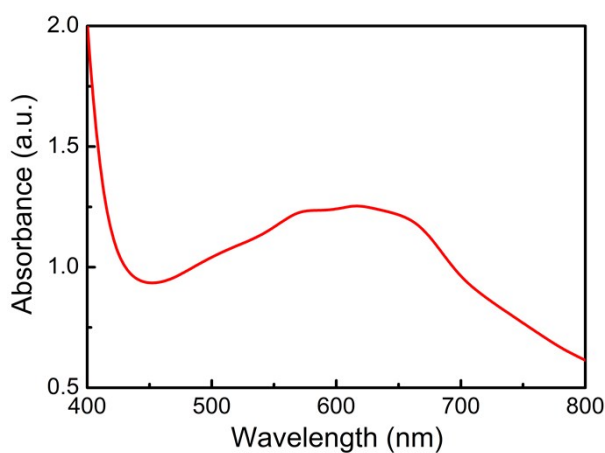


Figure S5: UV-Vis absorption spectrum of the aqueous solution of FeCl₃/CoCl₃ and tannic acid (Fe³⁺: Co³⁺: TA=1:1:6, pH=2)

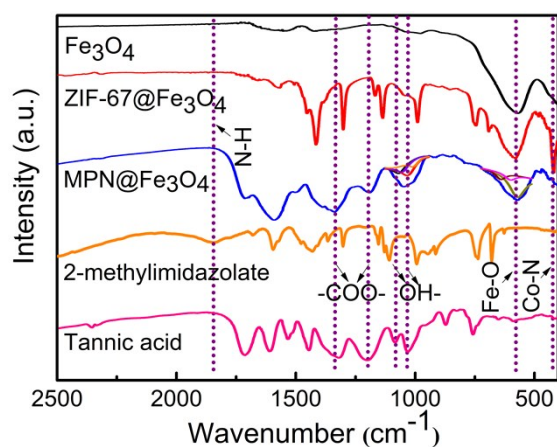


Figure S6: Comparison of the FT-IR spectra of MPN@Fe₃O₄ hybrid catalyst, ZIF-67@Fe₃O₄, Fe₃O₄, 2-methylimidazolate and tannic acid.

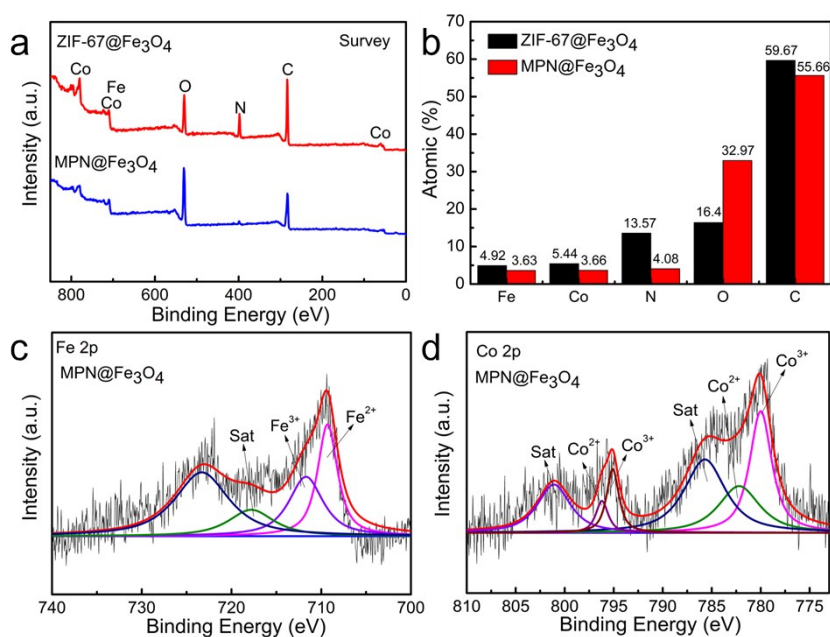


Figure S7: a) XPS survey spectra and (b) elemental concentration of ZIF-67@Fe₃O₄ and MPN@Fe₃O₄ hybrid particles. High-resolution XPS spectra of c) Fe 2p and d) Co 2p in MPN@Fe₃O₄

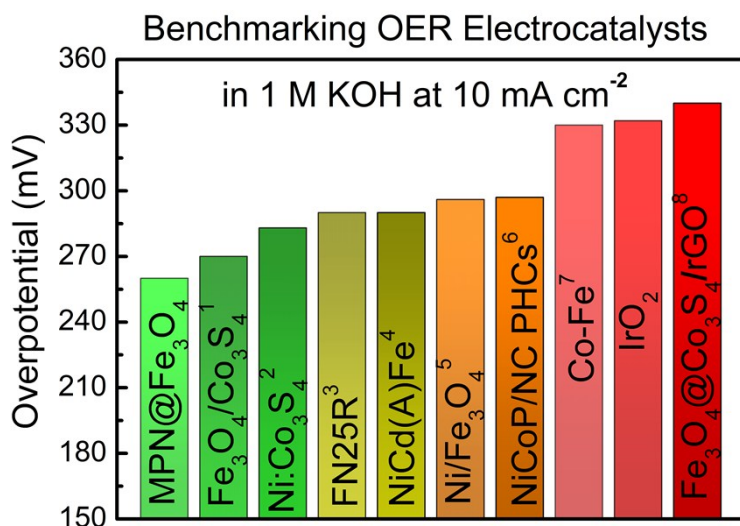


Figure S8: Comparison of the hybrid catalysts presented in this work with representative catalysts described in the literature. The comparison was based on their overpotential at the benchmark current density of 10 mA cm⁻².

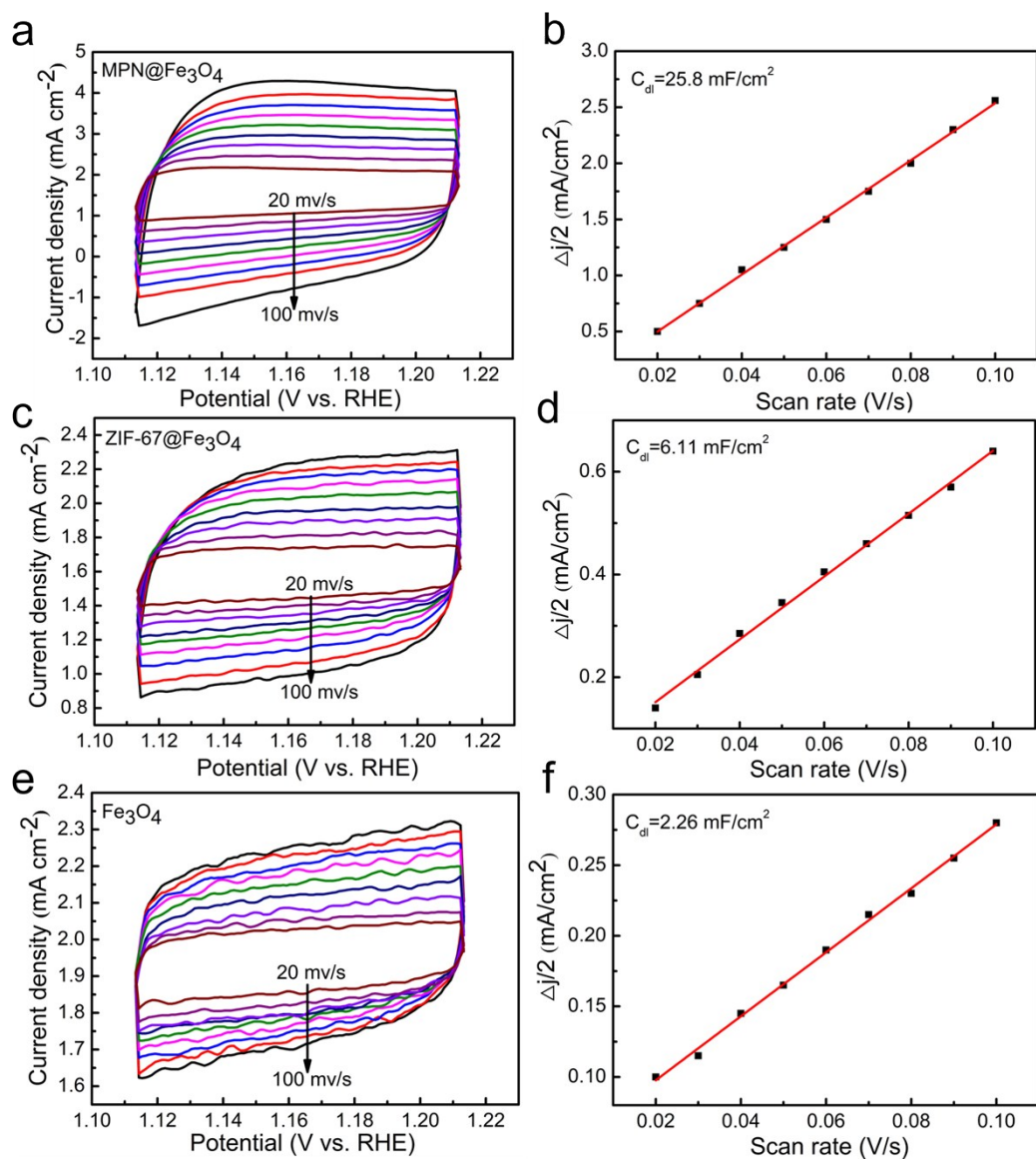


Figure S9: CV curves of a) MPN@Fe₃O₄, c) ZIF-67@Fe₃O₄ and e) Fe₃O₄ particles acquired at scan rates from 20 to 100 mV s⁻¹ in 1.0 M KOH; b), d), and f) are the relationship between the differences in current density vs scan rate from a), c) and e), respectively.

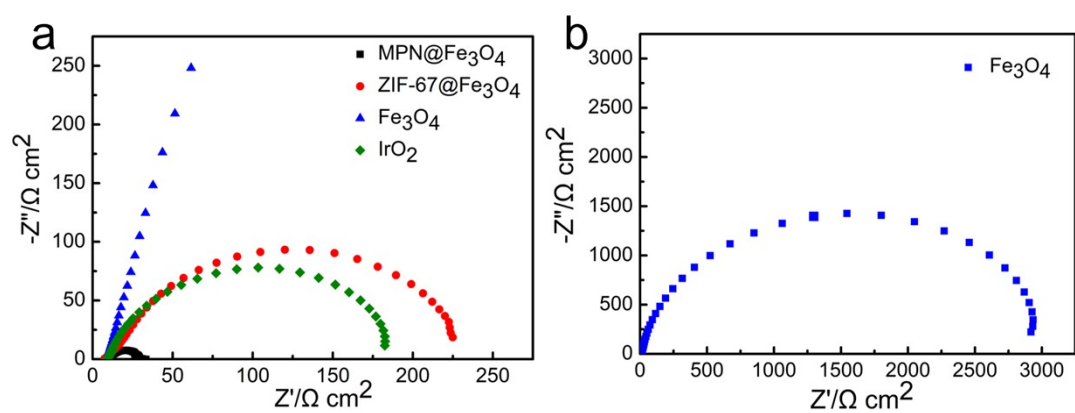


Figure S10: EIS of MPN@Fe₃O₄, ZIF-67@Fe₃O₄, Fe₃O₄ NPs and IrO₂.

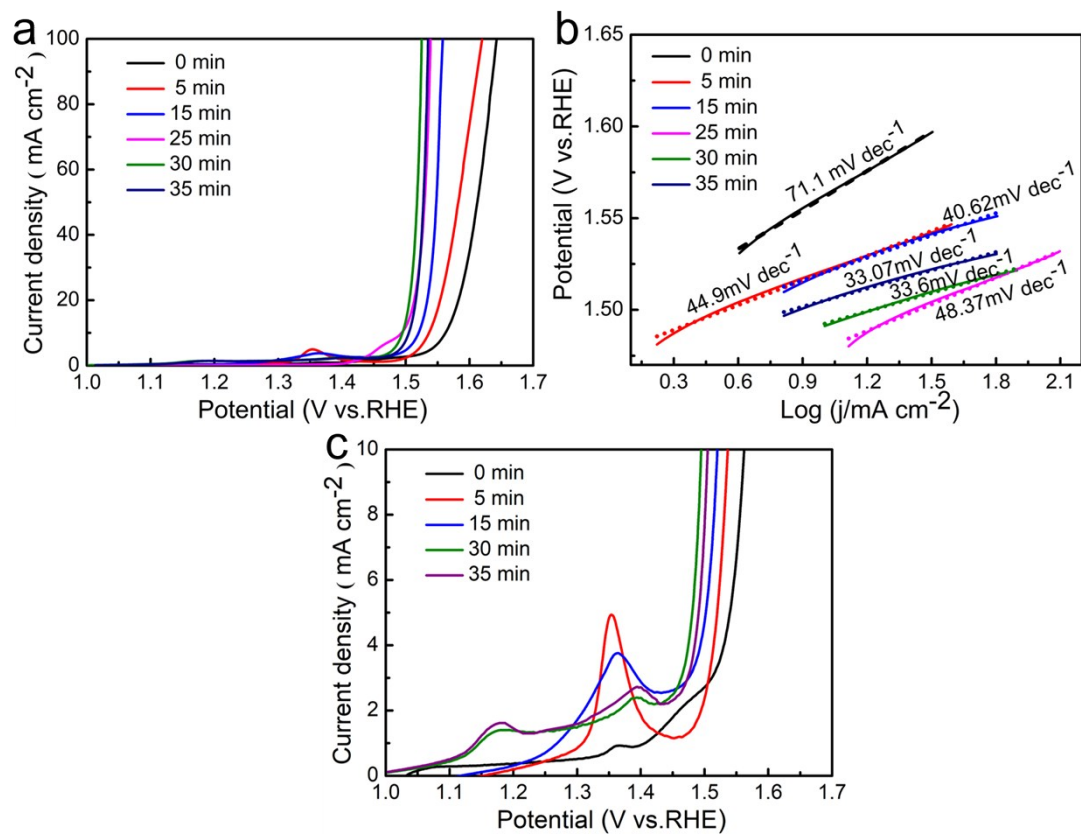


Figure S11: LSV and Tafel plot of MPN@Fe₃O₄ electrocatalysts prepared by varying the reaction time between tannic acid and ZIF-67@Fe₃O₄ as specified.

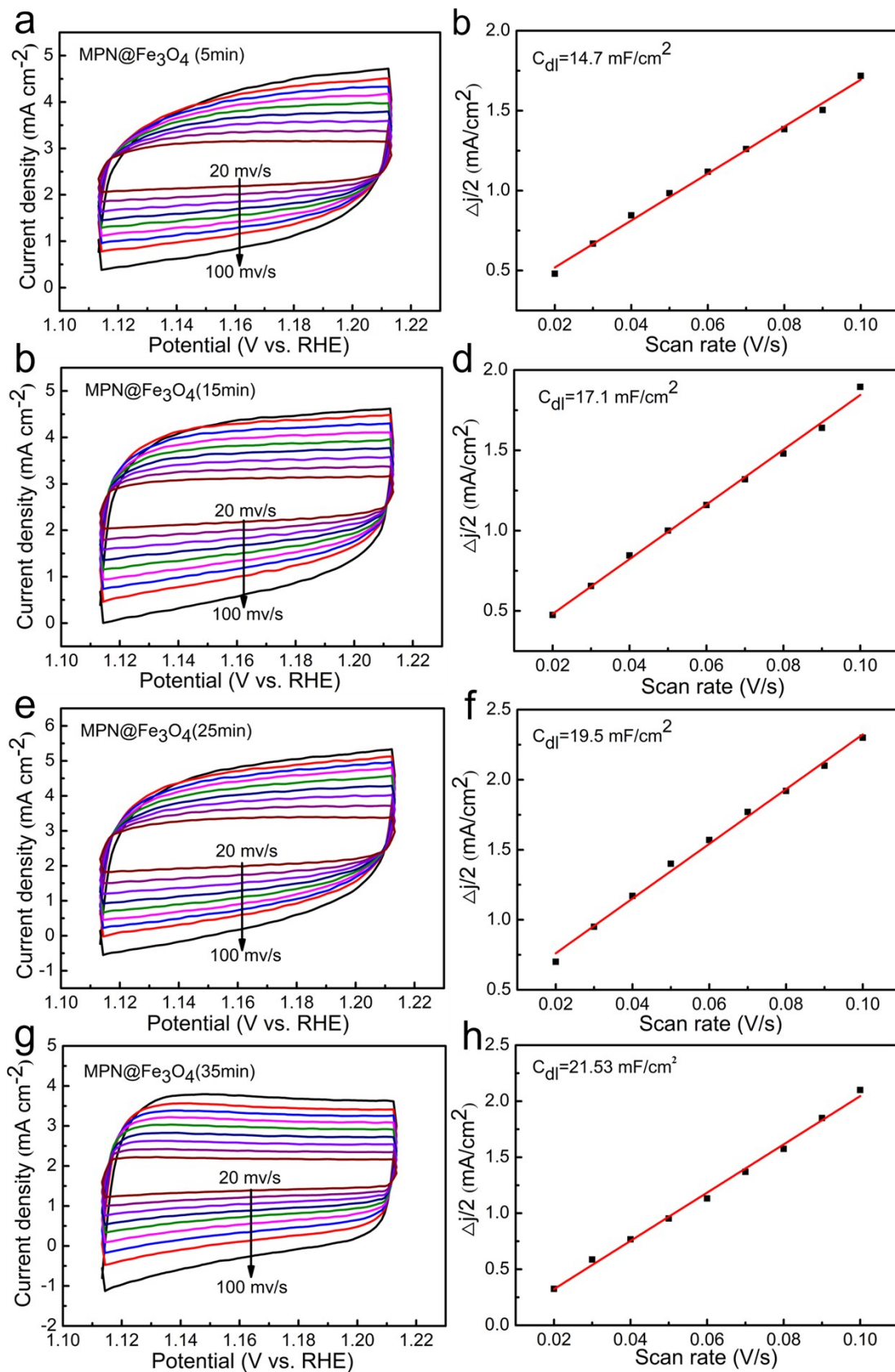


Figure S12. CV curves (left) and current-scan rate relationship (right) of MPN@Fe₃O₄ catalysts prepared by varying the reaction time between tannic acid and ZIF-67@Fe₃O₄.

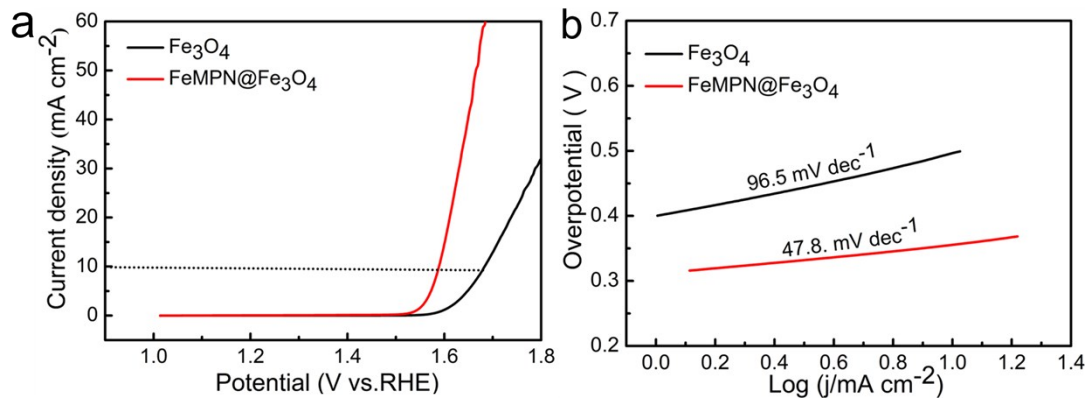


Figure S13: a) LSV and b) Tafel plot of pristine Fe_3O_4 and $\text{FeMPN@Fe}_3\text{O}_4$. The presence of FeMPN significantly improve the OER activity of Fe_3O_4 .

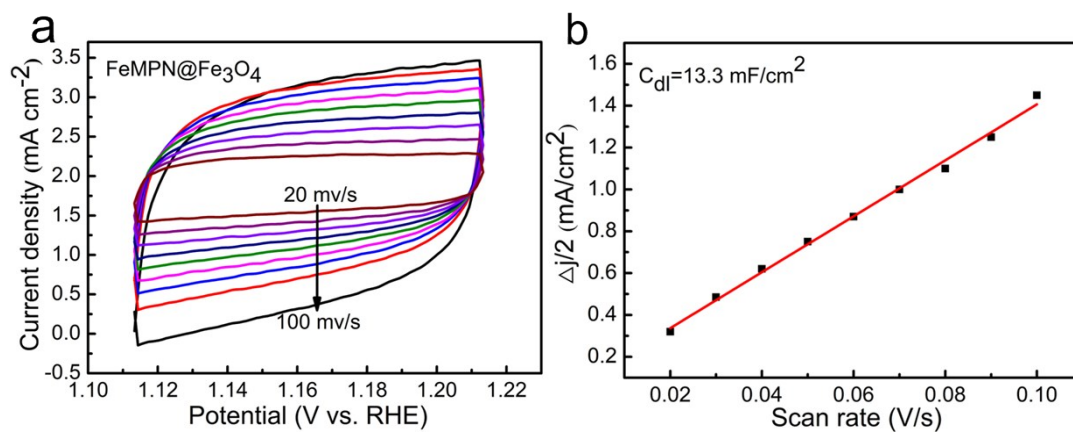


Figure S14: a) CV curves and b) current-scan rate relationship of $\text{FeMPN@Fe}_3\text{O}_4$ electrocatalysts.

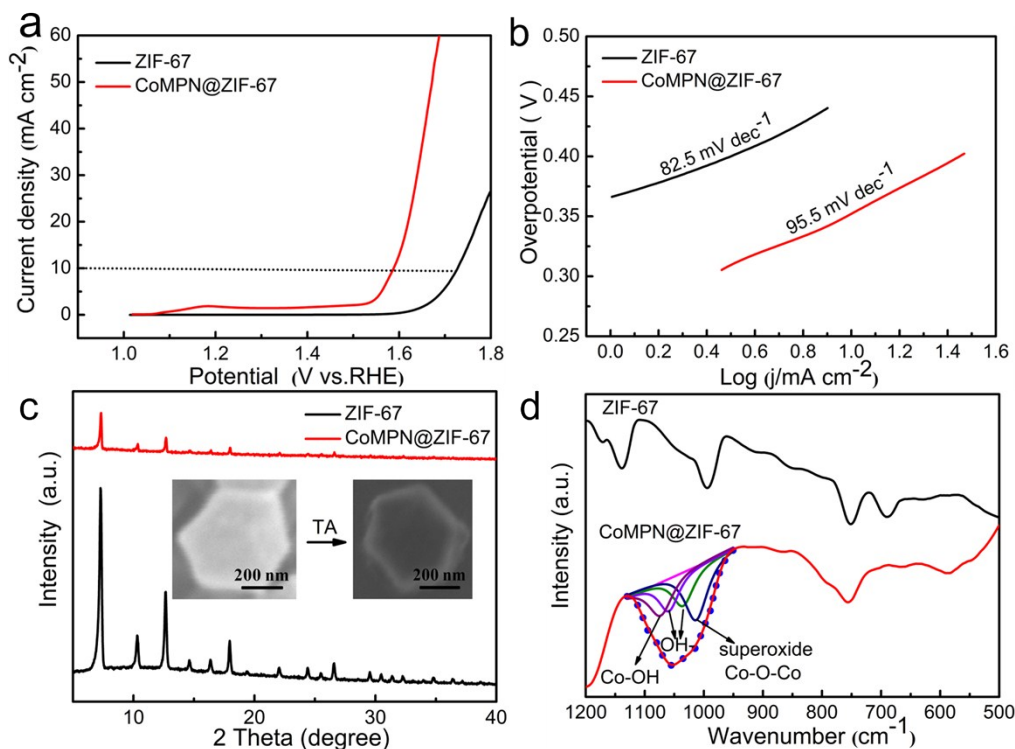


Figure S15: a) LSV and b) Tafel plot of pristine ZIF-67 and CoMPN@ZIF-67. The presence of CoMPN significantly improve the OER activity of ZIF-67. C) XRD pattern and SEM images, and d) FT-IR spectra of ZIF-67 and CoMPN@ZIF-67, the presence of thin organic MPN layers were evident.

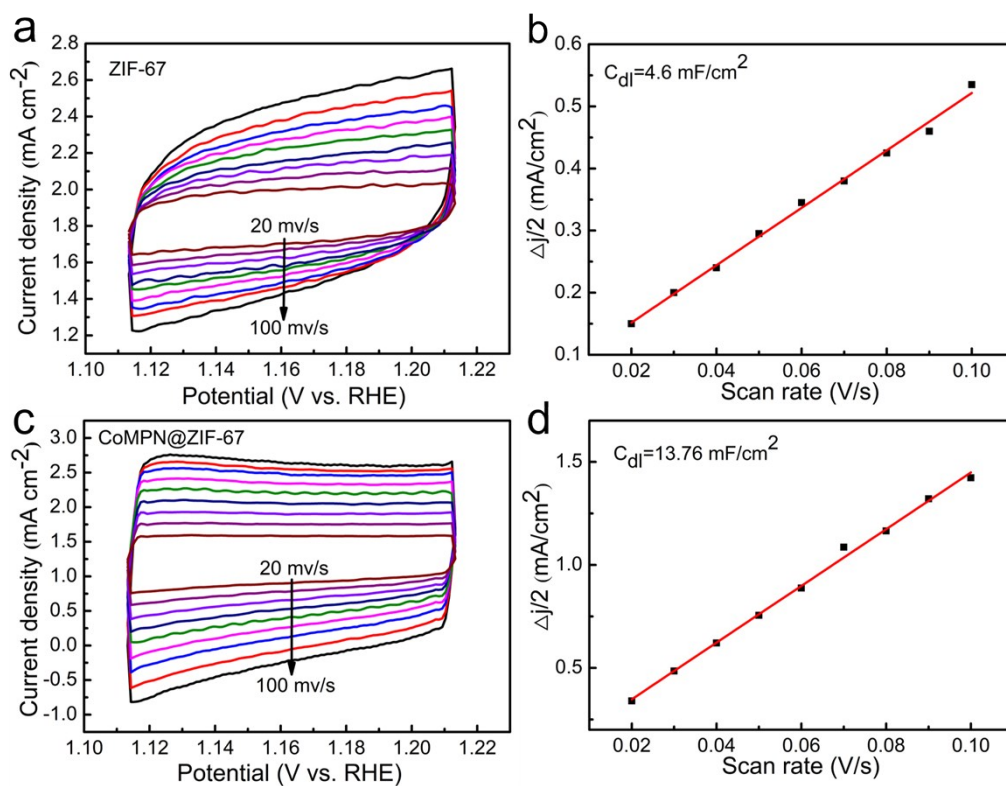


Figure S16: left) CV curves and right) current-scan rate relationship of a-b) ZIF-67 and c-d)

CoMPN@ZIF-67 electrocatalysts.

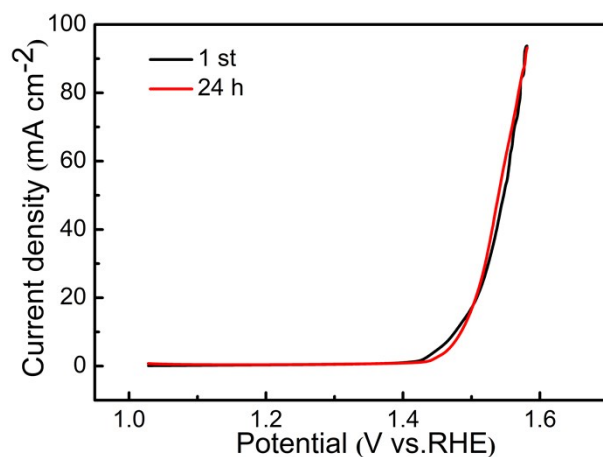


Figure S17: LSV of MPN@Fe₃O₄ hybrid catalysts before and after the durability test.

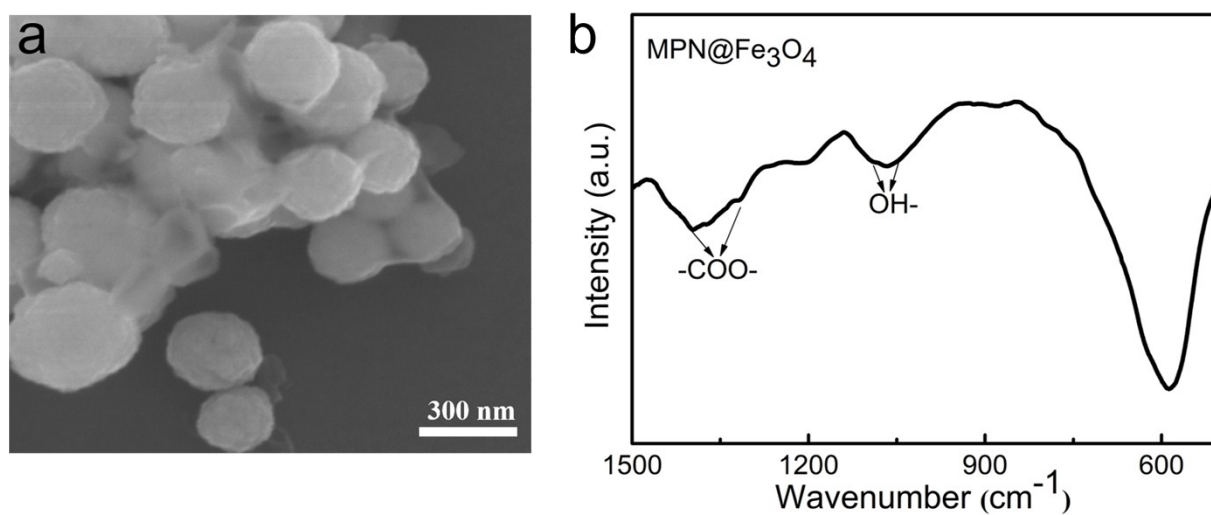


Figure S18: a) SEM image and b) FT-IR spectrum of MPN@Fe₃O₄ particles after the stability tests. No obvious morphological/spectral changes were observed

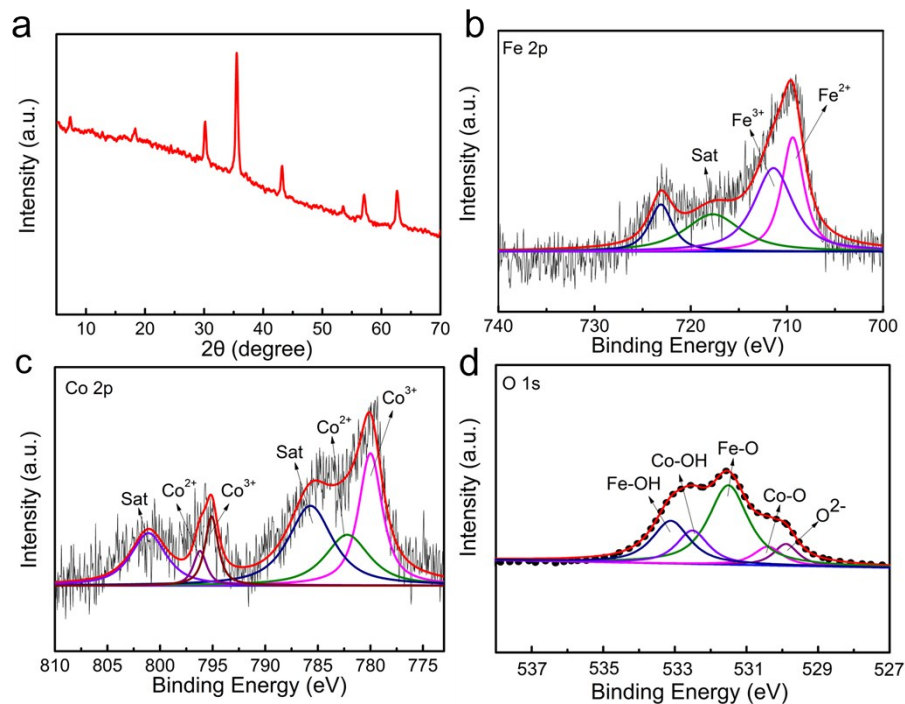


Figure S19: a) XRD pattern and high resolution XPS spectra of b) Fe 2p_{3/2}, c) Co 2p_{3/2}, and d) O 1s of MPN@Fe₃O₄ after durability test.

Reference

- 1 J. Du, T. Zhang, J. Xing and C. Xu, *Journal of Materials Chemistry A* 2017, **5**, 9210-9216.
- 2 J. H. Kim, D. H. Youn, K. Kawashima, J. Lin, H. Lim and C. B. Mullins, *Applied Catalysis B: Environmental*, 2018, **225**, 1-7.
- 3 W. Zhang, X. Jiang, X. Wang, Y. V. Kaneti, Y. Chen, J. Liu, J. S. Jiang, Y. Yamauchi and M. Hu, *Angew. Chem. Int. Ed. Engl.*, 2017, **56**, 8435-8440.
- 4 S. Xu, C. Lv, T. He, Z. Huang and C. Zhang, *Journal of Materials Chemistry A*, 2019, **7**, 7526–7532
- 5 G. Liu, R. Yao, Y. Zhao, M. Wang, N. Li, Y. Li, X. Bo, J. Li and C. Zhao, *Nanoscale*, 2018, **10**, 3997-4003.
- 6 X. Zhang, L. Huang, Q. Wang and S. Dong, *Journal of Materials Chemistry A*, 2017, **5**, 18839-18844.
- 7 M. Xiong and D. G. Ivey, *Electrochimica Acta*, 2018, **260**, 872-881.
- 8 J. Yang, G. Zhu and Y. Liu, *Advanced Functional Materials*, 2016, **26**, 4712-4721.